Article

Silymarin Alleviates Oxidative Stress and Inflammation Induced by UV and Air Pollution in Human Epidermis and Activates β-Endorphin Release through Cannabinoid Receptor Type 2

Cloé Boira [1],* , Emilie Chapuis [1], Amandine Scandolera [1] and Romain Reynaud [2]

1   Givaudan Active Beauty, 51110 Pomacle, France
2   Givaudan Active Beauty, 31400 Toulouse, France
*   Correspondence: cloe.boira@givaudan.com

Abstract: Background: Skin is exposed to ultraviolet radiation (UV) and air pollution, and recent works have demonstrated that these factors have additive effects in the disturbance of skin homeostasis. Nuclear-factor-erythroid-2-related factor 2 (Nrf2) and aryl hydrocarbon receptor (AHR) appear to be appropriate targets in the management of combined environmental stressors. The protective effects of silymarin (SM), an antioxidant and anti-inflammatory complex of flavonoids, were evaluated. Methods: Reactive oxygen species (ROS) and interleukin 1-alpha (IL-1a) were quantified in UV+urban-dust-stressed reconstructed human epidermis (RHE) treated with SM. A gene expression study was conducted on targets related to AHR and Nrf2. SM agonistic activity on cannabinoid receptor type 2 (CB2R) was evaluated on mast cells. The clinical study quantified the performance of SM and cannabidiol (CBD) in skin exposed to solar radiation and air pollution. Results: SM decreased morphological alterations, ROS, and IL-1a in UV+urban-dust-stressed RHE. AHR- and Nrf2-related genes were upregulated, which control the antioxidant effector and barrier function. Interleukin 8 gene expression was decreased. The clinical study confirmed SM improved the homogeneity and perceived well-being of urban skins exposed to UV, outperforming CBD. SM activated CB2R and the release of β-endorphin from mast cells. Conclusions: SM provides protection of skin from oxidative stress and inflammation caused by two major factors of exposome and appears mediated by AHR-Nrf2. SM activation of CB2R is opening a new understanding of SM's anti-inflammatory properties.

Keywords: UVA; UVB; pollutants; NQO1; filaggrin; keratin 16; interleukin 6

1. Introduction

As an interface between the body and environment, human skin is exposed to interrelated internal and external factors, described by the term "exposome", which contribute to the skin aging process [1]. Intrinsic or chronological aging describes the genetically determined process naturally occurring during the life span, which can be accelerated by environmental influences, which is called extrinsic aging [2]. Skin is particularly exposed to extrinsic aging, with UV and air pollution being major players of the skin aging exposome [1]. From 2009, Burke and Wei gathered evidence of synergistic damage caused by UVA and pollutants, increasing the risk of skin cancer [3]. Recent works reported the interplay between air pollutants and UV in the disturbance of skin redox homeostasis, inflammation, and barrier function alteration [4–6]. Ozone or particulate matter combined with UV demonstrate an additive effect in increasing markers of oxidation (lipid peroxidation, heme oxygenase-1 HO-1) and inflammation (transcription factor NFκB, cyclooxygenase 2 COX2) and in decreasing barrier-associated proteins (filaggrin, involucrin). Polycyclic aromatic hydrocarbons (PAHs) or particulate matter and UVA trigger a greater phototoxic effect than UV alone and are associated with reactive oxygen species (ROS) production and mitochondrial impairments.

ROS are continuously generated in living cells to ensure metabolism and act as intracellular messengers for cell and tissue homeostasis [2]. The maintenance of physiological redox status is controlled by endogenous regulators, notably nuclear-factor-erythroid-2-related factor 2 (Nrf2), which targets an array of antioxidant and detoxifying genes such as HO-1 and NAD(P)H quinone dehydrogenase 1 (NQO1) [7]. Nrf2 induces those genes by binding to a DNA motif called antioxidant response element (ARE).

UV, PAHs, volatile organic compounds, oxides, particulate matter, ozone, and cigarette smoke induce oxidative stress in skin and, combined with pollution exposure, have an additive effect in the activation of Nrf2 [8,9]. The alteration of the oxidative balance is the main driver of skin senescence, especially in the epidermis, where the ROS load is high [10,11]. ROS impair proteins, lipids, and DNA by direct oxidation, but also induce biological responses: degradation of dermal structural components (collagen, elastin) and secretion of inflammatory mediators through NFκB signaling. This direct relationship between oxidative stress and inflammation, which in return generate a pro-oxidative environment, can represent a chronic challenge for the organism exposed to daily environmental insults, called oxinflammation [12].

The aryl hydrocarbon receptor (AHR) is a xenobiotic chemical sensor, expressed in keratinocytes, fibroblasts, melanocytes, and T-cells. AHR mediates oxidative response, as well as the antioxidant pathway in a fine-tuned cross-talk with Nrf2 [13]. AHR's exogenous ligands include ozone, particulate matter, and PAHs [14]. After ligand binding in the cytosol, the AHR is translocated to the nucleus and dimerizes with the AHR nuclear translocator (ARNT) to bind to the xenobiotic-responsive element (XRE) of several genes, such as cytochrome P450 1A1 monooxygenase (CYP1A1), which can generate ROS and proinflammatory mediators. On the opposite side, natural compounds such as flavonoids bind to the AHR and activate the Nrf2-NQO1 pathway, which protects cells from ROS-induced oxidative damage. Another role of AHR signaling is the promotion of epidermal barrier function by upregulating genes involved in cornified cell envelop formation such as filaggrin (FLG) through the transcription factor OVO-like 1 (OVOL1) in keratinocytes [15].

Recent findings pointed out the interaction between the Nrf2 signaling pathway and cannabinoid receptor type 2 (CB2R) in different biological models, and it has been concluded that the Nrf2 signaling pathway's activation potentiates the effects of CB2R agonists [16–18]. CB2R activation reduces inflammatory cytokines and lesions in psoriasis models through the Nrf2 pathway and induces β-endorphin release in keratinocytes, so decreasing nociception [19,20].

Topical application of cosmeceuticals containing antioxidants appears an efficient strategy to prevent skin barrier damage induced by environmental stressors [5,10,21]. Silymarin (SM) is a seed extract of *Silybum marianum* (L.) Gaertn. (*Asteraceae*), commonly named milk thistle and renowned for its hepatoprotective properties. SM contains specific flavonoids called flavonolignans, mixing taxifolin and coniferyl alcohol moieties. Dermatological applications of SM are based on its antioxidant properties and protective effects against UV-induced skin damages [22]. Indeed, topical treatments containing SM inhibit photocarcinogenesis in a murine model and protect human keratinocytes from UVB-induced apoptosis and DNA damages [23]. SM's components also have anti-inflammatory properties and decrease the production of LPS-induced pro-inflammatory cytokines in keratinocytes [24]. SM and silibinin, its main constituent (50–70%), exert antioxidant properties at different levels: direct free radical scavenging; inhibition of specific enzymes responsible for free radical production; maintenance of mitochondrial integrity in stressed conditions; and activation of antioxidant enzymes and non-enzymatic antioxidants, mainly via transcription factors, including NFκB and Nrf2 [25,26].

The aim of this study was to explore the antioxidant and anti-inflammatory properties of SM in the context of skin's daily exposure to UV and urban air pollution. SM decreased ROS and IL-1a in RHE exposed to UV and urban dust. A gene expression study suggested the activation of Nrf2 and AHR, with antioxidant effector NQO1, and barrier-function-associated proteins filaggrin and keratin 16. SM induced CB2R and β-endorphin release. A

clinical study confirmed SM to improve the homogeneity and radiance of skin exposed to UV and air pollution and its positive psychological influence on volunteers' mood through self-evaluation, outperforming cannabidiol.

2. Materials and Methods

2.1. SM Composition

SM is a brownish-yellow powder obtained by ethyl-acetate extraction of *Silybum marianum* (L.) Gaertn. seeds. Quantitation of SM extract in silibinin equivalents was achieved by HPLC according to European Pharmacopeia quality control standards. Silibinin A and B, silicristin, silidianin, and isosilibinin A and B were quantified. The analysis was performed on a Lichrospher RP-18 125 × 4 mm, 5 μm (Merck, Darmstadt, Germany) maintained at 25 °C. The mobile phases were orthophosphoric acid 85%/methanol/water (0.5/35/65, v/v) and orthophosphoric acid 85%/methanol/water (0.5/50/50, v/v). The flow rate was 0.8 mL/min and the injection volume was 10 μL. Detection was performed in UV at 288 nm.

2.2. Impact of SM on Induced Oxidative Stress in NHEKs

The cell culture was performed on primary cells freshly isolated from biopsies. Normal human skin samples were collected from a donor who had given informed consent. Normal Human Epidermal Keratinocytes (NHEKs) were seeded in a black plate with a glass bottom at 20,000 cells per well in 96-well plates with a type I collagen pre-coating in quadruplicate. The cells were incubated for 24 h in complete medium (Dermalife medium supplemented with factors, Cell systems, Troisdorf, Germany) at 37 °C with 5% CO_2. Then, the cells were treated in complete medium supplemented with resveratrol (positive control) at 50 μM or SM at 0.001, 0.005, and 0.01 mg/mL. Skin cells cultivated in complete medium without supplementation were used as the negative control. After 24 h of incubation at 37 °C and 5% CO_2, the 2′,7′-Dichlorofluorescin diacetate (DCFH-DA) probe was added to the wells at 50 μM for at least 30–45 min at 37 °C. The cells were then washed two times with phosphate-buffered saline (PBS) and treated with the oxidative stress inducer, tert-Butyl hydroperoxide solution (TBP), at 5 mM in PBS. The untreated cells remained in the PBS. Finally, the emitted fluorescence was measured in darkness by an excitation wavelength at 488 nm and an emission wavelength at 525 nm with the microplate reader (TECAN). The study was carried out in quadruplicate (n = 4).

2.3. Impact of Urban Dust and UV Exposure on RHE Treated with SM

An 8-day-old reconstructed human epidermis (RHE-Lb) of 0.6 cm^2 was used for this test (Synelvia, Labège, France). Two products were tested: a formulation containing SM 1% (w/w) and the placebo cream (without SM). The RHEs were treated or not (negative control) with formulations, by topical application, and incubated for 24 h.

INCI formula: AQUA/WATER, CETYL ALCOHOL, GLYCERYL STEARATE, PEG-75 STEARATE, CETETH-20, STEARETH-20, ISODECYL NEOPENTANOATE, PENTYLENE GLYCOL, PHENOXYETHANOL.

At day 9, the product residue was removed with a swab. The RHEs were then placed in irradiation medium containing DCFH-DA and incubated for 1 h. After a medium change to remove DCFH-DA and a topical rinse, the RHEs were exposed to the UVA/B stress (UVA 2.5 J/cm^2 + UVB 100 mJ/cm^2) with or without urban dust (100 μg/mL, topical application, 50 μL/RHE) using BIO-SUN (Vilber, Collégien, France). Urban dust corresponded to particulate matter of a characterized composition: heavy metals (cadmium, lead, mercury, nickel, vanadium), aluminum, copper, chromium, manganese, chlorinated pesticides, polychlorinated Biphenyl (PCB) congeners, PAHs, nitro-PAHs, dibenzo-p-dioxin, and dibenzofuran congeners. Immediately after the stress, the RHEs were transferred to fresh assay medium (Epilife optimized by Synelvia) and incubated for 6 h applying the placebo, SM 1%, or no treatment, before being processed. Each RHE was cut into two parts. A half RHE was processed for histology, and a half RHE was processed for ROS quantification. The RHE media (subnatants) were collected and stored at −20 °C before

IL-1a quantification by ELISA or treatment of NHEKs for gene expression analysis. All experimental conditions were performed in triplicate (n = 3).

Histological analysis was conducted on fixed tissues, dehydrated in multiple baths with increasing concentrations of ethanol, and then, embedded in paraffin. Transversal sections were performed with a microtome (5 μm thickness, 1 slide per labeling) and maintained at room temperature. The sections were then deparaffinized and stained according to the standard protocol of hematoxylin eosin (HE) staining. Briefly, sections were stained with hematoxylin, rinsed, and stained with eosin. The sections were then rinsed and mounted in aqueous medium.

To achieve ROS quantification, the RHEs were embedded in optimal cutting temperature (OCT) medium and frozen at −80 °C until the blocks were processed for sectioning in a cryostat and mounted on slides. Tissue sections were observed using a ZEISS 710 confocal microscope. Images were captured and processed with ZEN software (objective lens ×20). The fluorescence intensity was quantified using the ImageJ software and normalized to the living layer area of the epidermis (i.e., excluding the stratum corneum) identified by DAPI staining of nuclei. Three image per replicate were captured.

Quantification of IL-1a in the RHE subnatants was performed according to the kit manufacturer's instructions (R&D Systems, Minneapolis, MN, USA # DY200-05, standard curve range: 7.8–500 pg/mL).

2.4. Gene Expression Study on NHEKs Treated with Stressed RHE Conditioned Medium

Keratinocytes were seeded in a 24-well plate and cultured for 24 h in culture medium, which was then replaced by assay medium containing, or not (control), the conditioned media of the RHEs for a further 24 h of incubation. The conditioned media were tested at 50%. The following experimental conditions were tested: stressed conditioned medium from non-treated the RHE stressed with UV and urban dust and stressed conditioned medium from the RHE stressed with UV and urban dust and treated with SM 1%. At the end of the incubation, the cells were washed in PBS solution and immediately frozen at −80 °C. All experimental conditions were performed in triplicate (n = 3).

Gene expression analysis was realized by the RT-qPCR method on total RNA extracted from the cell monolayers of each experimental condition. Total RNA was extracted from each sample using the TriPure Isolation Reagent® according to the supplier's instructions. The quality of the RNA was evaluated using capillary electrophoresis (Bioanalyzer 2100, Agilent technologies, Santa Clara, CA, USA). The quantity of the RNA was evaluated using a spectrophotometer (Synergy H1, BioTek Instruments, Winooski, VT, USA). The complementary DNA (cDNA) was synthesized by reverse transcription of the total RNA in the presence of oligo(dT) and "Transcriptor Reverse Transcriptase" (Roche, Basel, Switzerland). The cDNA quantities were then adjusted before the qPCR step. The qPCR was performed using a LightCycler® system (Roche Molecular Systems Inc., Basel, Switzerland) according to the supplier's instructions. The reaction mix (10 μL) was prepared as follows: 2.5 μL of cDNA, primers (forward, reverse) and reagent mix (Ozyme, Saint-Cyr-l'Ecole, France) containing Taq DNA polymerase, SYBR Green I, and $MgCl_2$. The reference gene Actin Beta (ACTB) was used for data normalization.

2.5. Activation of Human CB2R by CBD or SM: EC50 Determination

The activation of the CB2R was evaluated on human recombinant CB2R. Several concentrations of CBD or SM or 100 nM of WIN 55212-2, a CB2R agonist, or no treatment (control) were applied during 10 min at 37 °C, and cAMP was measured by HTRF to evaluate the EC50. The EC50 values (concentration producing a half-maximal response) were determined by non-linear regression analysis of the concentration–response curves generated with the mean replicate values using Hill equation curve fitting, where Y = response, A = left asymptote of the curve, D = right asymptote of the curve, C = compound concentration, C_{50} = EC50, and nH = slope factor.

$$Y = D + \frac{A - D}{1 + \left(\frac{C}{C_{50}}\right)^{nH}}$$

This analysis was performed using software developed at Cerep (Hill software) and validated by comparison with data generated by the commercial software SigmaPlot® 4.0 for Windows® (©1997 by SPSS Inc., Chicago, IL, USA). The cellular agonist effect was calculated as a percentage of control agonist response (WIN 55121-2) for each target, and the cellular antagonist effect was calculated as a percentage of the inhibition of the control reference agonist response for each target.

2.6. Activation of Human CB2R by CBD or SM in Mast Cells and β-Endorphin Release

Human mast cells (HMC1.1) were isolated from fresh skin biopsies (SCC097, Sigma-Aldrich, St. Louis, MO, USA) and treated for 16 h with CBD at 0.0025 mg/mL or SM at 0.05 mg/mL (*w/v*). Cells were then incubated at 37 °C, 5% CO_2. After 16 h, the supernatant was collected for further ELISA analysis, and the cells were collected and counted with a Luna cell counter. The release of cAMP and β-endorphin by the mast cells was quantified using ELISA kits and following the supplier's recommendation (Abcam, Cambridge, UK).

2.7. Clinical Study: Impact of SM on Urban Skins and Comparison with Cannabidiol

A double-blind, placebo-controlled clinical study was carried on 68 women aged between 45 and 75 years old. All the subjects participating gave their informed consent, signed at the beginning of the study. The study followed and was in compliance with the tenets of the Declaration of Helsinki. The volunteers are living in a dense urban environment in Thailand and are, thus, exposed both to UV rays and pollution (Spincontrol Asia, Bangkok, Thailand). The volunteers applied a placebo formula or formula with SM 1% or formula with CBD 0.02% twice a day for 56 days.

The INCI formula composition was as follows: AQUA, CETHYL ALCOHOL, GLYCERYL STEARATE, PEG-75 STEARATE, CETETH-20, STEARETH-20, PENTYLENE GLYCOL, ISODECYL NEOPENTANOATE, +/− SILYBUM MARIANUM FRUIT EXTRACT, CAPRYLIC/CAPRIC TRIGLYCERIDE, CITRIC ACID, DIMETHICONE, SODIUM BENZOATE, AMMONIUM ACRYLOYDIMETHYLTAURATE/BEHENETH-25 METHACRYLATE CROSSPOLYMER, FRAGRANCE, +/− CANNABIDIOL 99%.

The inclusion criteria for the recruitment of the panelists were: being female subjects, being 45–75 years of age, being exposed to UV rays and pollution several times a day, including all skin types with at least 1 subject by skin type, having sensitive skin based on the stinging test, having underneath eye wrinkles with a grade ≥ 4 according to the Skin Atlas (p. 47), and having dull complexion according to the C.L.B.T. scale from Spincontrol Asia.

Digital photography using VISIA CR2.3® was performed to analyze skin homogeneity and radiance, and the volunteer completed a Well-Being Questionnaire analyzed by Emospin (Emospin, Tours, France). The Well-being Questionnaire (W-BQ) was originally constructed to measure psychological well-being in people with a chronic somatic illness. Because of its versatility and robustness, this tool is recommended by the World Health Organization for widespread use [27].

2.8. Statistical Analysis

For the *in vitro* and *ex vivo* studies, a Shapiro–Wilk normality test was performed to evaluate whether the data followed the Gaussian Law. If the results had a normal distribution, a Student's *t*-test statistical analysis was performed. If the results did not follow the Gaussian Law, a non-parametric statistical analysis was performed by Kruskal–Wallis ANOVA followed by the Mann–Whitney U test.

All raw data from the *in vivo* experiments were analyzed by the Shapiro–Wilk test in order to determine if the data followed the Gaussian Law or not. If yes, the data were analyzed using a parametric paired or unpaired Student's *t*-test. If not, the data were

analyzed using the non-parametric Wilcoxon test or the non-parametric Mann–Whitney test. Self-assessment was analyzed by the contingency method using the Chi-squared test with ** $p < 0.01$.

A result was considered as significant if $p < 0.1$ #, $p < 0.05$ *, $p < 0.01$ **, and $p < 0.001$ ***.

3. Results

3.1. SM Composition

SM is a standardized extract of *Silybum marianum* (L.) Gaertn. seeds, enriched in flavonolignans. In this study, the main phenolic compounds were identified as silibinin A and B, constituting 56% of the SM. As previously reported [22], the studied SM also contained minor flavonolignans: silicristin and silidianin representing 30.3% of the extract and isosilibinin A and B, 13.8%.

3.2. SM Reduced ROS during Oxidative Stress on NHEKs

ROS are generated as a first response to environmental stressors in skin [28]. SM has oxidant scavenging properties and decreases UV-induced oxidative stress [22,23]. Here, this activity was observed on the NHEk model treated with the oxidative stress inducer, TBP, at 5 mM. In TBP-treated NHEKs, the amount of ROS significantly increased by 82% (Figure 1). Pretreatment with a positive antioxidant control, resveratrol, led to a reduction in the ROS by 63% compared to TBP-treated cells. SM at 0.001 mg/mL did not modify the ROS quantity. SM at 0.005 mg/mL and 0.01 mg/mL significantly reduced the ROS in a dose-dependent manner, −16% and −34%, respectively, compared to the TBP treatment condition. Preliminary studies demonstrated that SM 0.01 mg/mL did not impact cell viability in the MTT assay (3-(4,5-dimethylthiazol-2-yl)-2,5-diphenyltetrazolium bromide) with 90% of viability vs. the non-treated condition. These data confirm that SM has antioxidant properties in epidermal cells.
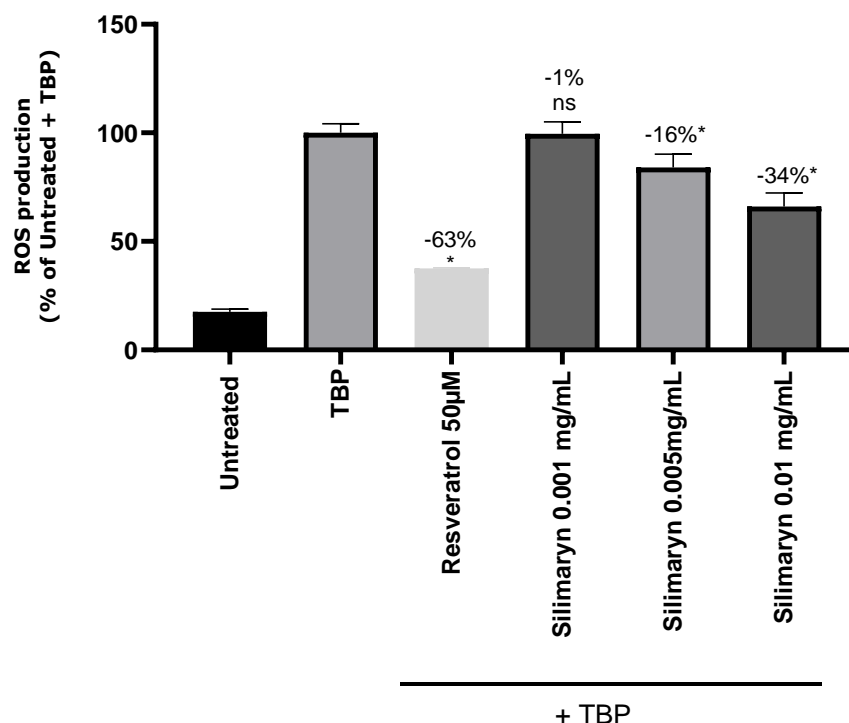

Figure 1. Quantification of reactive oxygen species (ROS) in normal human epidermal keratinocytes (NHEKs) without treatment (untreated), treated with tert-Butyl hydroperoxide (TBP) 5 mM, and pretreated with resveratrol 50 μM (positive control) or silymarin (SM) at 0.001 mg/mL, 0.005 mg/mL, or 0.01 mg/mL before TBP application. Results are expressed as a percentage of the condition stressed with TBP. Mann–Whitney test, ns: not significant and $p < 0.05$ *.

3.3. SM Maintains Normal Phenotype on UVA/B+Urban-Dust-Stressed RHEs

The additive effect of UV and air pollutants was previously demonstrated [4,5]. The RHEs were treated with SM 1% in formulation or placebo before and after exposure to UVA/B and urban dust. Morphological change analysis and ROS and IL-1a quantification allowed the comparison of the untreated, placebo, and SM conditions.

The morphological analysis is presented in Figure 2. The control RHE (untreated) exhibited a normal phenotype characterized by a multi-layered epidermis showing tissue differentiation from the basal layer to the *stratum corneum* with the presence of many grains of keratohyalin in the granular layer. Tissues stressed with UVA/B and urban dust were disorganized and exhibited a pathological morphology presenting pycnotic nuclei and spongiosis (intercellular edema), especially in the basal layer. The topical application of SM decreased pycnotic nuclei and spongiosis, while the placebo had no impact on the phenotype induced by UVA/B and urban dust exposure.
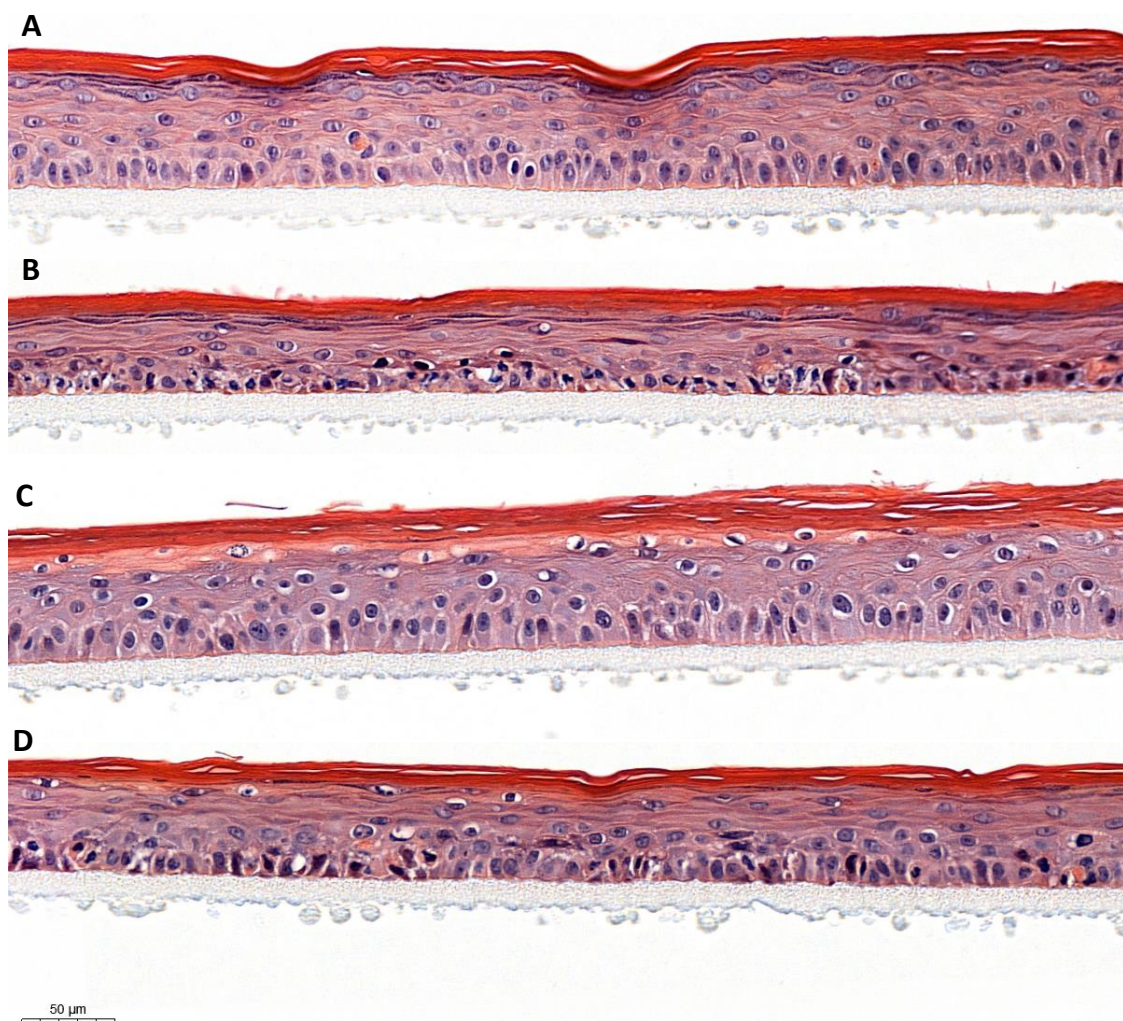

Figure 2. Comparison of reconstructed human epidermis (RHE) morphology: untreated control (**A**), exposed to UVA/B and urban dust (**B**), treated with silymarin 1% (**C**) or placebo (**D**) by topical application before and after exposure to UVA/B and urban dust.

3.4. SM Reduced ROS on UVA/B+Urban-Dust-Stressed RHEs

ROS were quantified in the RHEs in order to evaluate the oxidative stress induced by UVA/B and urban dust application and confirmed the antioxidant properties of SM. Representative pictures of the ROS analysis by fluorescence confocal microscopy are presented in Figure 3, and quantitative data are charted in Figure 4. The exposure of the RHEs to UVA/B

and urban dust increased the ROS content by +539% compared to the untreated condition. The placebo-treated RHE exhibited a similar increase in ROS content. Applying SM at 1% in the cream significantly reduced the ROS production by −295% vs. the untreated stressed condition. The results confirmed the ability of SM to reduce the ROS production in epidermis under combined exposure to common daily environmental stress.
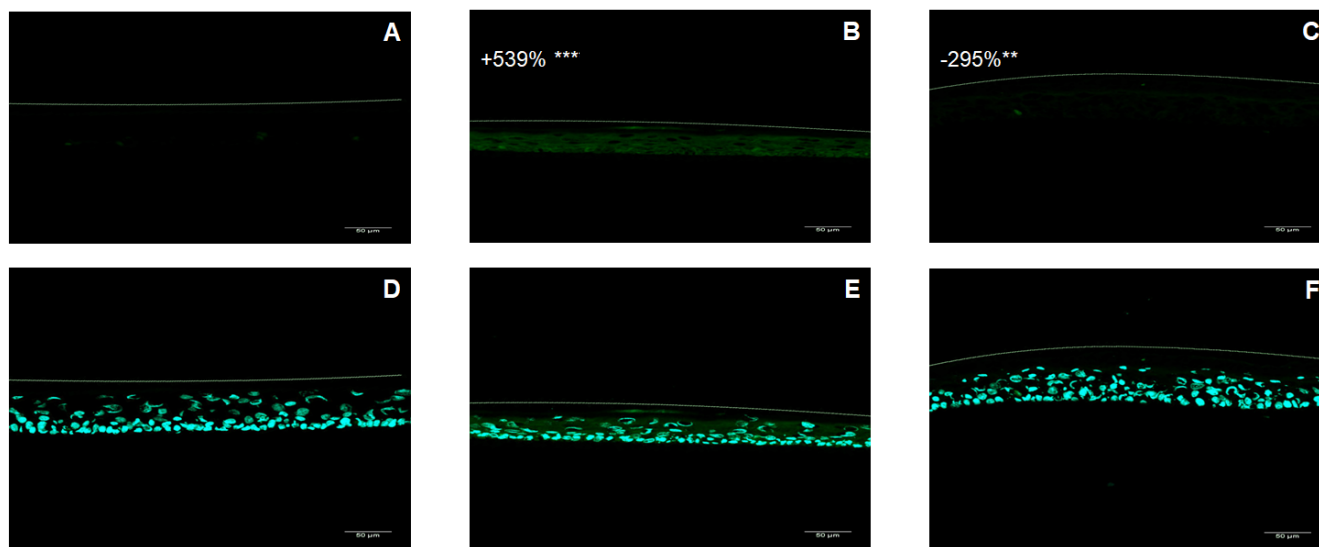

Figure 3. Representative pictures of fluorescence confocal microscopy for reactive oxygen species detection by dichlorofluorescein (DCF) (**A–C**) and 4′,6-diamidino-2-phenylindole (DAPI) staining (**D–F**) in untreated reconstructed human epidermis (RHE) (**A,D**), stressed with UVA/B and urban dust (**B,E**), and treated with the formulation containing silymarin 1% (**C,F**). The percentage is expressed in comparison to the unstressed control except for the silymarin-treated condition, for which a decrease is expressed in comparison to UVA-/B- and urban-dust-stressed condition. Mann–Whitney U test, $p < 0.01$ ** and $p < 0.001$ ***.
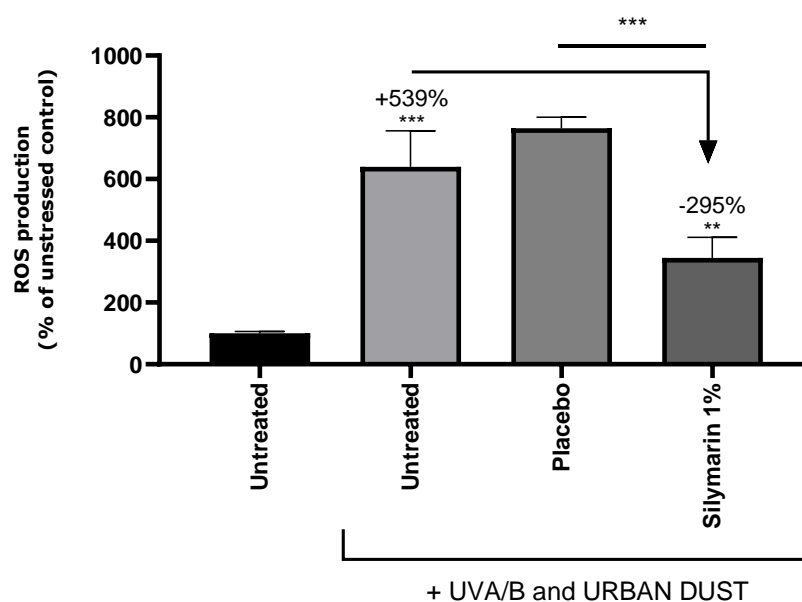

Figure 4. Quantification of reactive oxygen species in untreated reconstructed human epidermis, stressed with UVA/B and urban dust, and treated with the placebo cream or formulation containing silymarin 1%. The percentage is expressed in comparison to the unstressed control, except for the silymarin-treated condition, for which a decrease is expressed in comparison to the UVA-/B- and urban-dust-stressed condition. Mann–Whitney U test, $p < 0.01$ ** and $p < 0.001$ ***.

3.5. SM Reduced IL-1a on UVA/B+Urban-Dust-Stressed RHE

IL-1a is a pro-inflammatory cytokine highly expressed in the skin and produced by keratinocytes. It is considered as a key player in initiating the development of the inflammatory response [29]. Stress induced by UVA/B and urban dust increased the quantity of IL-1a in the subnatants of the RHE by +213% (Figure 5). Similar values were obtained on the subnatants of the RHE treated with the placebo formulation. The SM 1% cream decreased the IL-1a amount compared to the untreated stressed RHE by −81%. These data confirmed that SM has anti-inflammatory properties in this context.
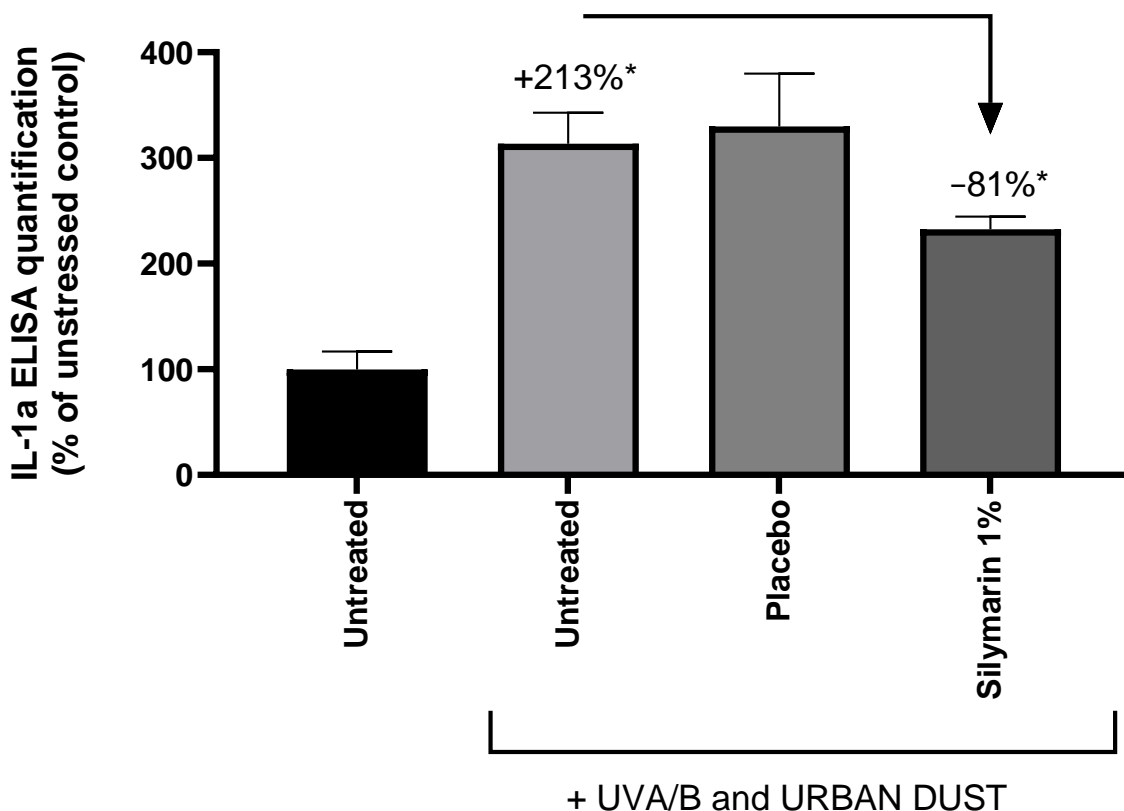

Figure 5. Quantification of interleukin 1 alpha (IL-1a) by enzyme-linked immunosorbent assay (ELISA) in untreated reconstructed human epidermis, stressed with UVA/B and urban dust, and treated with the placebo cream or formulation containing silymarin 1%. The percentage is expressed in comparison to unstressed control except for Silymarin treated condition, for which a decrease is expressed in comparison to the UVA-/B- and urban-dust-stressed condition. Mann–Whitney U test, $p < 0.05$ *.

3.6. SM Upregulated AHR and Nrf2 Pathways

In order to understand the mode of action of SM that underlies its antioxidant and anti-inflammatory properties, the conditioned medium of the stressed RHE treated with SM was used to stimulate NHEKs. A gene expression study was conducted to determine the genes that were upregulated or downregulated compared to the stimulation by the conditioned medium from the untreated stressed RHE (Figure 6).

Th interleukin 8 gene (IL-8), encoding a chemokine produced during oxidative stress induced by UV rays and pollutants, was significantly downregulated. The interleukin 6 gene (IL-6), encoding a pro-inflammatory cytokine, was close to being significantly downregulated. The expression of *CYP1A1*, coding for a monooxygenase involved in the detoxication of carcinogens through the AhR pathway, was not modified by the SM treatment.
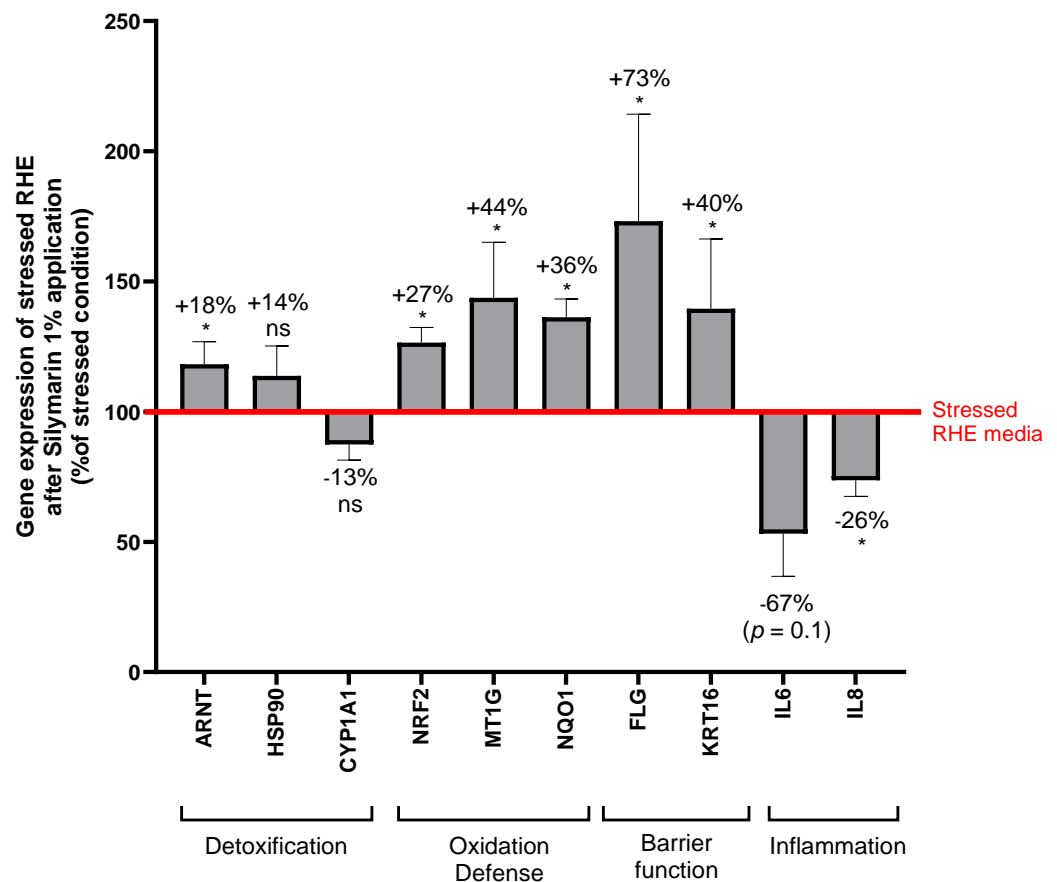
Figure 6. Relative gene expression of normal human keratinocytes treated with the conditioned medium of the stressed reconstructed human epidermis (RHE) treated with silymarin 1% before and after exposure to UVA/UVB and urban dust. Values are relative to the conditioned medium of the stressed RHE without treatment. *ARNT*: AhR nuclear translocator, *HSP90*: heat shock protein 90, *CYP1A1*: cytochrome P450 1A1 monooxygenase, *NRF2*: nuclear-factor-erythroid-2-related factor 2, *MT1G*: metallothionein 1G, *NQO1*: NAD(P)H quinone dehydrogenase 1, *FLG*: filaggrin, *KRT16*: keratin 16, *IL-8*: interleukin 8, *IL-6*: interleukin 6. Mann–Whitney U test, ns: not significant, and $p < 0.05$ *.

　　　Six genes were significantly upregulated, which encode the following proteins: ARNT complexing AhR in the nucleus; nuclear factor Nrf2 regulating oxidative stress and inflammation; NQO1, a target gene of Nrf2, regulating the cellular redox state through quinone detoxification; metallothionein 1G (MT1G), involved in the response to metallic ions; filaggrin (FLG), a structural protein involved in epidermal barrier function; and finally keratin 16 (KRT16), a type I keratin associated with wound repair, proliferation, and inflammation.

　　　These results indicate that SM potentially activated the AHR pathway without inducing its target *CYP1A1*. The increased expression of *FLG* and *KRT16* indicates a regulation of the epidermal barrier function by the plant extract. This is consistent with the AHR and Nrf2 activation: AHR regulates FLG through the transcription factor OVO-like 1 (OVOL1) in keratinocytes, and Nrf2 controls KR16 [15,30]. Upregulation of *FLG* and *KRT16* is also in accordance with the maintenance of a normal epidermal morphology in the SM-treated RHE. The Nrf2 pathway was also probably activated, as demonstrated by the upregulation of *Nrf2* and *NQO1*. The *MT1G* promoter contains the antioxidant response element [31], suggesting it could be regulated by Nrf2, and this reinforces our hypothesis. The decrease of IL-8 and IL-6 expression was expected as they are regulated by IL-1a [32,33], and this tends to confirm the anti-inflammatory activity of SM.

3.7. SM Activated Human CB2R

A recombinant human CB2R was used to test the ability of SM to reduce the release of cAMP and, so, activate CB2R, *in vitro*. A comparison with CBD was made. The EC50 of the reference agonist WIN55212-2 was 9.93×10^{-5} µg/mL. The EC50 of SM was determined at 76.0 µg/mL and that of CBD at 55.4 µg/mL, demonstrating a moderate agonist effect of both compounds on CB2R.

3.8. SM Activated CB2R in Mast Cells and Induced β-Endorphin Release

Mast cells are immune cells having an important role in the first-line defense of skin and in the regulation of barrier function [34,35]. They express CB2R, as keratinocytes, and appeared as a good model to test the potential SM agonist's effect [36]. Both SM and CBD activated the receptor (Figure 7).
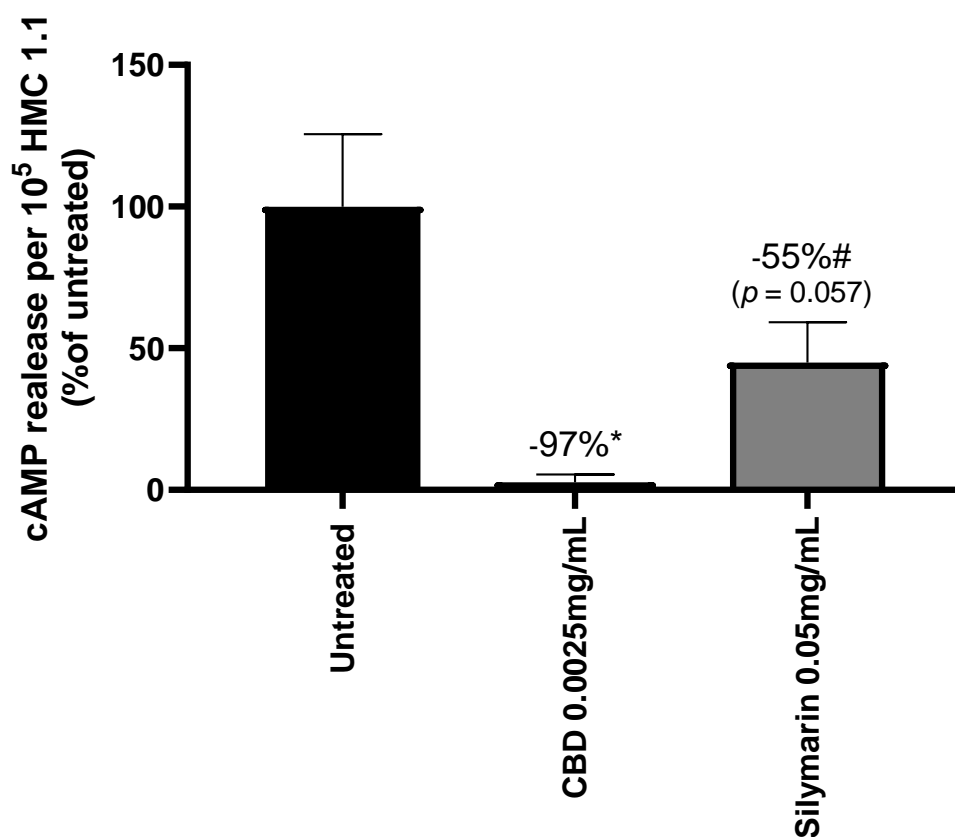

Figure 7. Activation of cannabinoid receptor type 2 (CB2R) in mast cells (HMC1.1) measured through the inhibition of cAMP release by cannabidiol (CBD) and silymarin. Results are expressed as a percentage of the untreated cells. Mann–Whitney test, $p < 0.1$ # and $p < 0.05$ *.

Ibrahim et al. demonstrated that CB2R activation in keratinocytes led to the release of β-endorphin [20]. This endogenous opioid was quantified in mast cells treated with CBD or SM in the presence or absence of a CB2R antagonist, SR144528, to confirm that β-endorphin release depends on CB2R activity. Both CBD and SM increased β-endorphin release from mast cells by +17% and +19%, respectively, compared to untreated cells. The use of the SR144528 CB2R antagonist did not modify β-endorphin release from CBD-treated mast cells, while it decreased by −23% in SM-treated mast cells (Figure 8). This confirmed that the SM activity on β-endorphin secretion is correlated with CB2R activation, which was not verified for CBD.
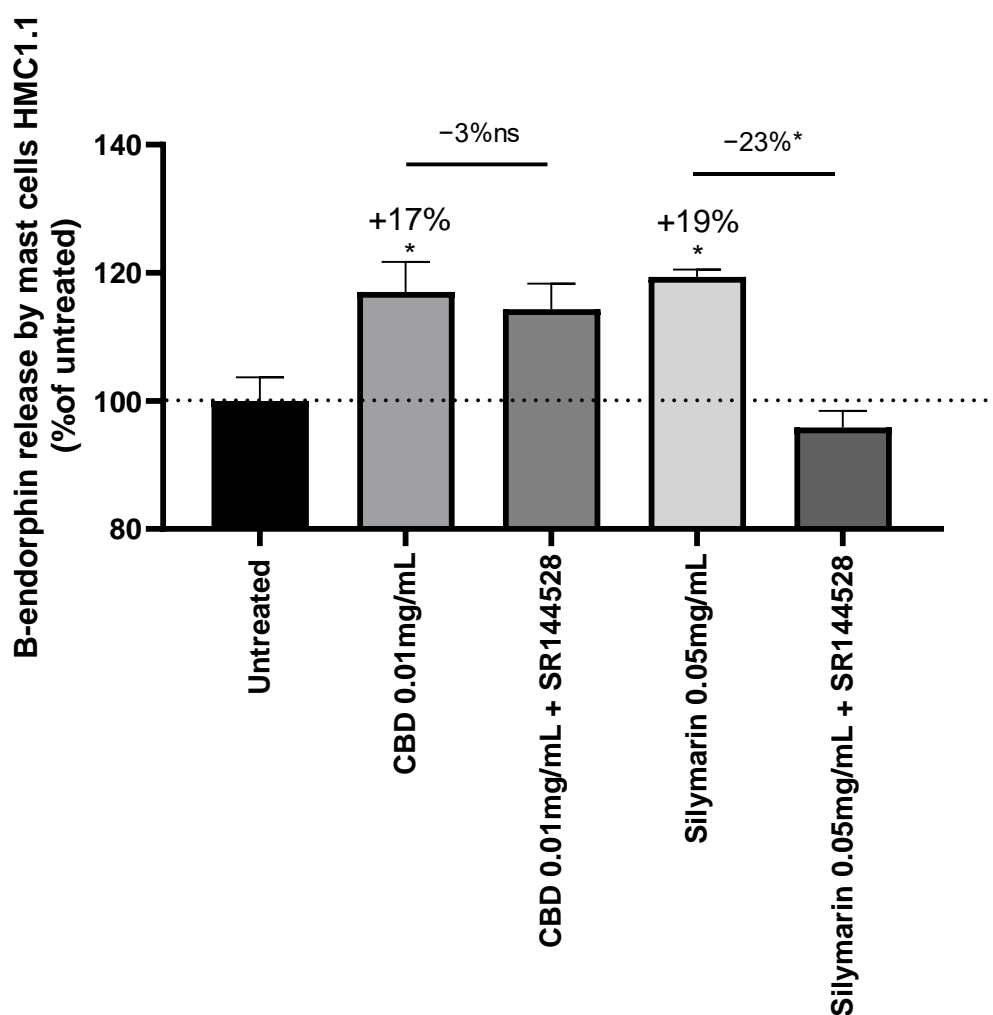
Figure 8. Quantification of β-endorphin (B-endorphin) release by mast cells (HMC1.1) induced by cannabidiol (CBD) and silymarin. SR144528 is a CB2R antagonist. The results are expressed as a percentage of the untreated cells' response. The decrease of β-endorphin release in CBD/SR144528 and silymarin-/SR144528-treated cells is expressed relative to CBD- and silymarin-treated cells. Mann–Whitney test, ns: not significant and $p < 0.05$ *.

3.9. SM Improved the Homogeneity and Radiance of Skins Exposed to UV and Air Pollution

A double-blind vs. placebo clinical study was conducted on 68 women, 45 to 75 years old, exposed daily to UV rays and air pollution, presenting sensitive skin and dull complexion according to the coloring, luminosity, brightness, and transparency (C.L.B.T.) scale. Placebo cream or formulation containing 0.02% CBD or 1% SM, were applied twice a day for 56 days. Skin homogeneity and radiance were evaluated at the last day of application. A Well-Being Questionnaire allowed measuring the impact of the actives on panelists' energy perception.

CBD activates antioxidant pathways regulating inflammation in keratinocytes, mediates epidermal differentiation through AHR signaling [37,38], and is considered as a potential therapeutic for inflammatory skin disorders [39]. CBD is today commercialized as a cosmetic active fighting inflammation and oxidative stress in sensitive skins. That is why CBD was selected as a benchmark for this study.

Skin homogeneity, defined as facial skin color distribution and skin smoothness in texture, was measured at day 56 and compared to day 0 (Figure 9). SM 1% induced an increase in skin homogeneity vs. day 0, by a factor of 1.6 compared to the placebo and by factor of 2.7 compared to CBD. On top of that, skin homogeneity improvement was effective in 91% of panelist using the SM formula, 52% of panelists using the CBD cream, and 72%

of panelists applying the placebo. These results are illustrated by representative pictures of the panelist applying the SM-containing cream (Figure 10A): the blue spots indicate that heterogeneous areas were attenuated along the study course, showing improvement in skin smoothness and color homogeneity; changes were not conspicuous for panelists applying CBD or placebo formulations (Figures 10B and 10C, respectively). The measurement of skin radiance (Figure 9) supported the findings on skin homogeneity: only SM 1% in the cream helped to significantly improve skin luminosity ($\times$1.6 vs. CBD).
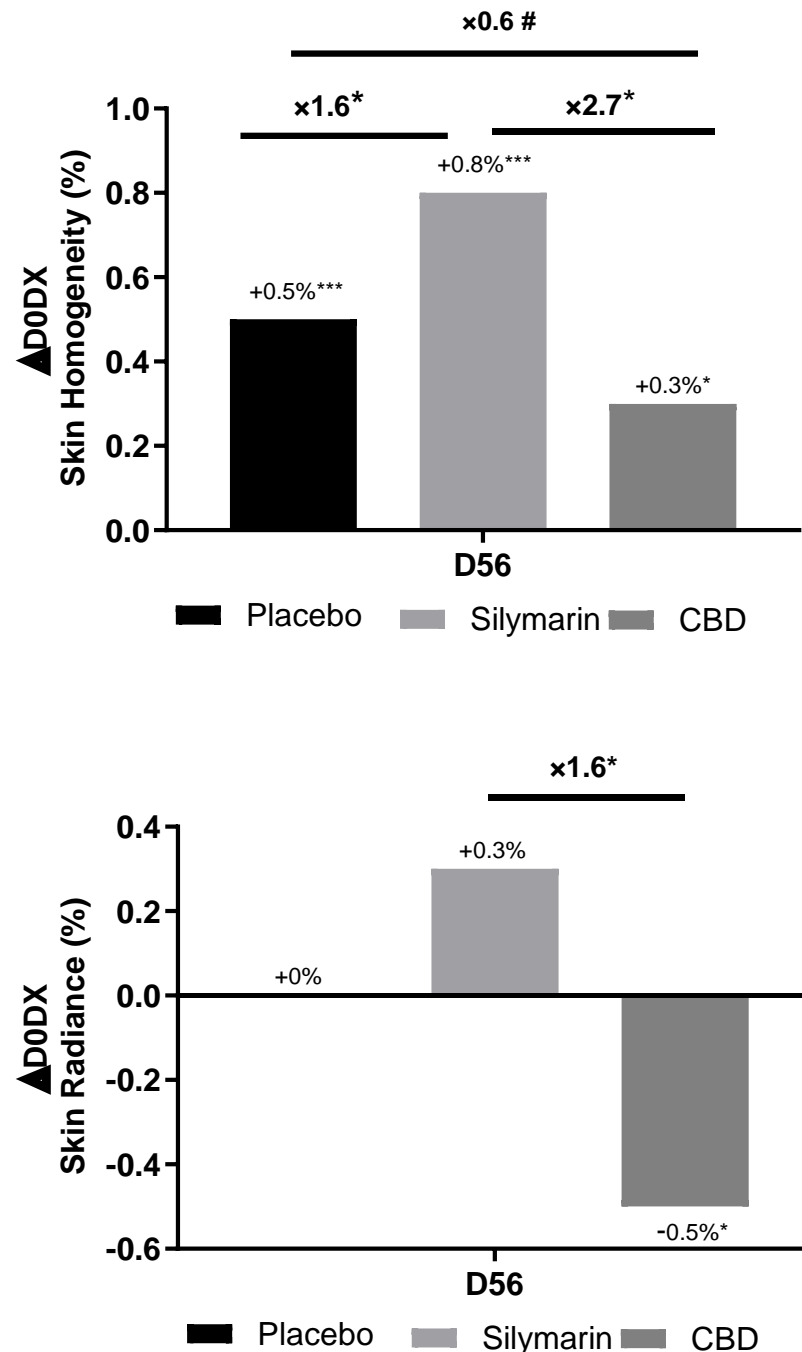

Figure 9. Comparison of skin homogeneity (**up**) and radiance (**down**) at day 56 (D56) vs. day 0 (D0) between the groups applying the placebo cream or silymarin 1% in formulation or cannabidiol (CBD) 0.02% in formulation. Wilcoxon test vs. D0, Mann–Whitney test vs. placebo, $p < 0.1$ #, $p < 0.05$ * and $p < 0.001$ ***.
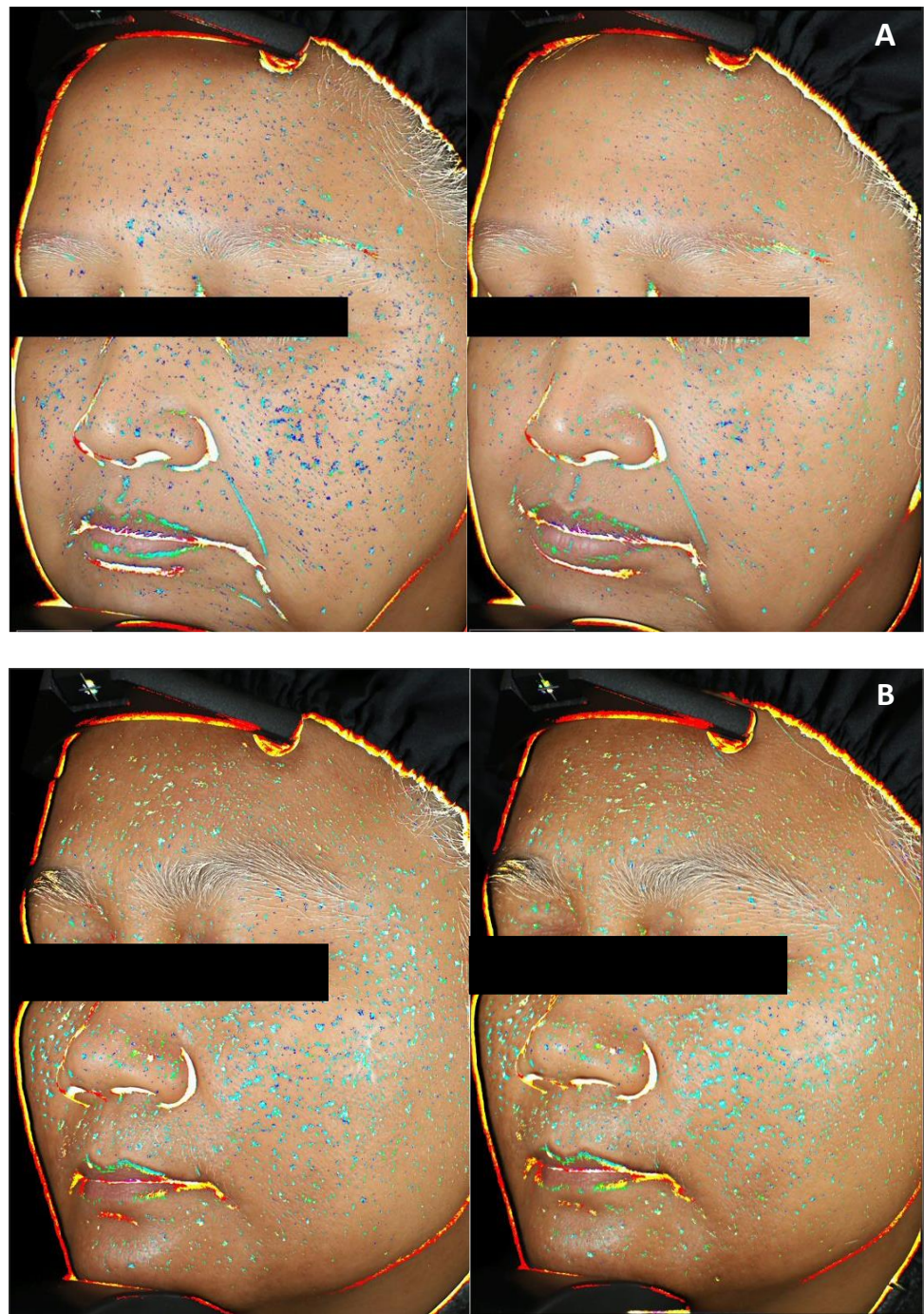
Figure 10. *Cont.*

Figure 10. Representative pictures illustrating skin homogeneity changes at day 0 (**left**) and day 56 (**right**) of the panelists applying silymarin 1% in formulation (**A**), or cannabidiol 0.02% in formulation (**B**), or placebo cream (**C**). Heterogeneity is indicated by blue spots: light blue representing the highest contrast to dark blue representing the lowest contrast.

The volunteers completed a Well-Being Questionnaire analyzed by Emospin. SM significantly improved energy well-being, in other words, a positive mood dynamic, in a similar manner as the cannabidiol compared to the placebo (Figure 11).
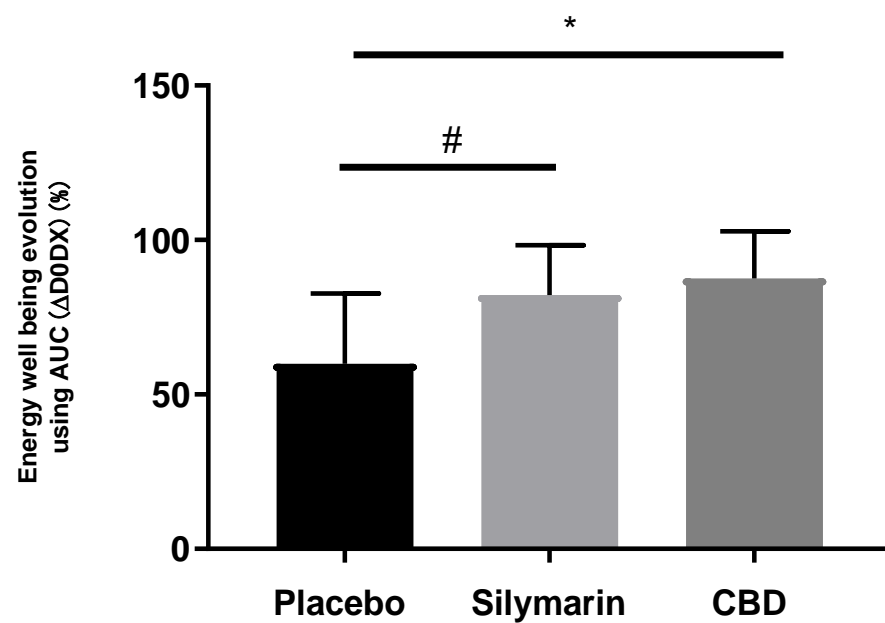

Figure 11. Quantitative data extracted from Well-Being Questionnaire and comparing the evolution of volunteers' self-evaluation of their skin energy. Mann–Whitney test vs. placebo, $p < 0.1$ #, and $p < 0.05$ *.

4. Discussion

Skin is particularly exposed to ultraviolet radiation (UV) and air pollution, which are major players in the skin aging exposome [1]. Recent works have demonstrated the interplay between air pollutants and UV in the disturbance of skin redox homeostasis, inflammation, and barrier function alteration, resulting in oxinflammation [4–6].

In our study, RHEs stressed by a combination of UV and urban dust presented morphological alterations, with increased ROS and IL-1a contents, suggesting oxidative stress and inflammation. IL-1a is constitutively secreted as precursor protein in keratinocytes and rapidly increases under UVB exposure, inducing the release of IL-6, IL-8, and inflammatory responses [32,33]. In the double-stressed RHE, SM maintained a normal tissue organization, decreased ROS and IL-1a, as well as the expression of IL-6 and IL-8. Frankova et al. suggested that the anti-inflammatory properties of SM are at least supported by silibinin, a major flavonolignan of SM, which tend to decrease IL-1a, IL-8, and IL-6 during SDS-induced inflammation in RHE.

Nrf2 is a master regulator of cellular antioxidant defenses, and its activation appears to be an interesting strategy to prevent skin from the damages caused by combined exposure to pollution and sun [40]. Indeed, Nrf2 mediates the induction of a set of detoxifying and antioxidant enzymes such as NQO1 by binding a DNA sequence called the antioxidant response element (ARE) [7]. Moreover, oxidative stress is mediated by a fine-tuned cross-talk between AHR and Nrf2 modulated by antioxidant phytochemicals divided into three groups: Nrf2 agonist with AHR agonistic activity, Nrf2 agonist with AHR antagonistic activity, and NrF2 agonist with CYP1A1 inhibitor activity [13]. According to our results, the antioxidant activity of SM was associated with an upregulation of Nrf2 and NQO1, together with genes involved in AHR activation (ARNT), suggesting agonistic activity on both pathways, and did not modify CYP1A1 expression. SM seems to belong to the group of Nrf2 agonist with AHR agonistic activity, including in soybean tar, *Opuntia ficus-indica* extract, *Houttuynia cordata* extract, and *Bidens Pilosa* extract, all containing high flavonoid content, like SM. Flavonoids are present in several dietary sources, and about 6000 structures have been identified. These phenolic compounds are clearly identified as Nrf2 activators [41] and, today, attract attention for the prevention and treatment of neurodegenerative disorders, cancer, or COVID-19 [42–44]. A structural activity relationship study among flavonoids for Nrf2 induction would be of particular interest to determine the effect of the peculiar structure of SM flavonolignans combining taxifolin and coniferyl alcohol.

Under UV and urban dust stress, SM was observed to increase the expression of genes encoding barrier-function-associated proteins, filaggrin and keratin 16. Indeed, UV is reported to decrease filaggrin content in the epidermis, and this effect is aggravated and prolonged by the combination with particulate matter exposure [5]. Filaggrin is genetically mapped to the epidermal differentiation complex (EDC) locus, comprising genes encoding proteins involved in the terminal differentiation and cornification of keratinocytes [45]. EDC genes' expression, including filaggrin, is modulated by UV and pollutants themselves, activating the AHR and accelerating keratinocytes differentiation via the OVO-like 1 transcription factor [15]. Keratin 16 is transiently expressed in keratinocytes under Nrf2 activation, in the event of a barrier breach, and regulates epithelial inflammation and keratinocytes proliferation, serving wound repair [30,46]. Collectively, these data support the hypothesis of AHR and Nrf2 activation by SM. Several studies have reported the direct cross-talk between the AHR and Nrf2: the AHR binding the xenobiotic-responsive element (XRE) of Nrf2 or the latter interacting with the cap'n'collar-small MAF binding element of the AHR promoter. An indirect way involves the AHR-induced expression of cytochrome P450, releasing intermediate metabolites and, then, oxidative stress, triggering NrF2 [47].

Recent findings have established evidence for the interaction of CB2R and Nrf2. The CB2R promoter region contains the ARE element and is effectively regulated by Nrf2 in microglial cells [16]. Agonists of CB2R induce Nrf2 in skeletal muscle [17], and a murine obesity model with an anti-inflammatory effect [48]. In diabetic mice, Nrf2 activation potentiates the effect of the CB2R agonist [18].

In skin, CB2R is mainly localized in cutaneous nerve fiber bundles, mast cells, and, to a lesser extent, epidermal keratinocytes [36]. CB2R activation stimulates the release of β-endorphin from keratinocytes, which acts at local neuronal μ-opioid receptors to inhibit nociception [20]. CB2R deficiency exacerbates psoriasis symptoms, and its agonists improve lesions and decrease inflammatory cytokines and oxidative stress through Nrf2 [19,49]. The anti-inflammatory properties of CB2R have also been confirmed in the skin wound healing process [50]. CBD is a major compound of *Cannabis sativa* L., which does not show psychoactivity, but has the potential to treat skin disorders due to its antioxidative and anti-inflammatory properties, as previously reviewed [39,51]. CBD reduces oxidative stress in normal human keratinocytes and induces CB2R, which is also promoted by UVA and UVB [52]. Moreover, UV-stressed 2D and 3D skin models exhibit cytoprotective response when treated with CBD [53].

We hypothesized that part of the anti-inflammatory activity of SM could be related to CB2R's induction. In a first assay, SM was shown to be a weak agonist of human CB2R, similar to CBD. Further tests were conducted on mast cells, which appeared as an appropriate model, as they play a key role in immunity and microbiota management thanks to the AHR [34], in the maintenance of epidermal barrier function [35], and some evidence suggests the role of CB2R in immune modulatory effects during inflammation [50,54]. Very interestingly, SM was found to activate CB2R and induced the release of β-endorphin from mast cells in a similar way as CBD. This opens a new area of research on the understanding of the anti-inflammatory and antioxidant properties of SM.

Solar radiation and air pollution cause premature ageing through several clinical signs: pigmentary changes including lentigines, wrinkles, roughness, skin pores, skin redness, rosacea, and altering skin homogeneity [28]. A radiant complexion means healthy and young skin and influences facial attractiveness [55,56]. SM significantly improved skin homogeneity for 91% of the volunteers, who felt a positive impact on their energy well-being, reflecting a more-radiant and healthier skin compared to the volunteers applying the CBD formula. The scientific literature was previously reviewed that has established CBD's activities, explaining its growing interest and use in the cosmetic industry: antioxidant, anti-inflammatory, β-endorphin inductor, skin redness reduction, and mood enhancer [57]. Finally, in the tested conditions, SM appeared as efficient as CBD to promote CB2R and β-endorphin in mast cells and better improved the sensitive skin condition on women exposed to UV and air pollution.

5. Conclusions

This study reports SM's protective effects against the consequences of combined exposure to UV and air pollution. By reducing oxidative stress and inhibiting pro-inflammatory cytokines, SM preserved the oxinflammation balance. SM's bioactivity appeared to be mediated by AHR and Nrf2 signaling. A clinical study confirmed that SM improves urban skins' complexion and is an alternative to CBD. As a new finding, SM activated CB2R in mast cells and the release of β-endorphin, opening a new lead in the understanding of the anti-inflammatory mechanisms of the flavonoid complex.

Author Contributions: Conceptualization, C.B., A.S. and R.R.; methodology, C.B., E.C., A.S. and R.R.; validation, C.B., E.C., A.S. and R.R.; formal analysis, C.B. and E.C.; investigation, C.B.; writing—original draft preparation, C.B.; writing-review and editing, C.B., E.C., A.S. and R.R. All authors have read and agreed to the published version of the manuscript.

Institutional Review Board Statement: The study was conducted in accordance with the Declaration of Helsinki and did not meet the criteria requiring evaluation by an ethics committee. According to French regulations, it does not meet the criteria requiring evaluation by an ethics committee. Indeed, according to French regulations, the evaluation of a cosmetic ingredient does not require approval from an ethics committee. However, the clinical study is conducted in accordance with good laboratory practices and the Helsinki agreements, and provides the following information: (1) A

toxicology certificate regarding the applied formulas. (2) A protocol describing the research objective, inclusion and exclusion criteria, measurement methods used, volunteer recruitment methods, methods of anonymizing volunteers, and methods of collecting and securing personal data. (3) Informed consent is provided to each volunteer. It describes the study objective and the means employed in an understandable manner, as well as compensation and emergency contact numbers. Only protocols involving "interventional" analysis methods are subject to ethical approval in France. The study mentioned in this article does not require this because no "interventional" measures are performed.

Informed Consent Statement: Informed consent was obtained from all subjects involved in the study.

Data Availability Statement: The original contributions presented in the study are included in the article, further inquiries can be directed to the corresponding author.

Conflicts of Interest: The authors declare no conflicts of interest.

References

1. Krutmann, J.; Bouloc, A.; Sore, G.; Bernard, B.A.; Passeron, T. The Skin Aging Exposome. *J. Dermatol. Sci.* **2017**, *85*, 152–161. [CrossRef] [PubMed]
2. Rinnerthaler, M.; Bischof, J.; Streubel, M.K.; Trost, A.; Richter, K. Oxidative Stress in Aging Human Skin. *Biomolecules* **2015**, *5*, 545–589. [CrossRef] [PubMed]
3. Burke, K.E.; Wei, H. Synergistic Damage by UVA Radiation and Pollutants. *Toxicol. Ind. Health* **2009**, *25*, 219–224. [CrossRef] [PubMed]
4. Soeur, J.; Belaïdi, J.-P.; Chollet, C.; Denat, L.; Dimitrov, A.; Jones, C.; Perez, P.; Zanini, M.; Zobiri, O.; Mezzache, S.; et al. Photo-Pollution Stress in Skin: Traces of Pollutants (PAH and Particulate Matter) Impair Redox Homeostasis in Keratinocytes Exposed to UVA1. *J. Dermatol. Sci.* **2017**, *86*, 162–169. [CrossRef] [PubMed]
5. Ferrara, F.; Woodby, B.; Pecorelli, A.; Schiavone, M.L.; Pambianchi, E.; Messano, N.; Therrien, J.-P.; Choudhary, H.; Valacchi, G. Additive Effect of Combined Pollutants to UV Induced Skin OxInflammation Damage. Evaluating the Protective Topical Application of a Cosmeceutical Mixture Formulation. *Redox Biol.* **2020**, *34*, 101481. [CrossRef]
6. Ferrara, F.; Pambianchi, E.; Woodby, B.; Messano, N.; Therrien, J.-P.; Pecorelli, A.; Canella, R.; Valacchi, G. Evaluating the Effect of Ozone in UV Induced Skin Damage. *Toxicol. Lett.* **2021**, *338*, 40–50. [CrossRef]
7. Ma, Q. Role of Nrf2 in Oxidative Stress and Toxicity. *Annu. Rev. Pharmacol. Toxicol.* **2013**, *53*, 401–426. [CrossRef]
8. Puri, P.; Nandar, S.K.; Kathuria, S.; Ramesh, V. Effects of Air Pollution on the Skin: A Review. *Indian J. Dermatol. Venereol. Leprol.* **2017**, *83*, 415–423. [CrossRef]
9. Cervellati, F.; Woodby, B.; Benedusi, M.; Ferrara, F.; Guiotto, A.; Valacchi, G. Evaluation of Oxidative Damage and Nrf2 Activation by Combined Pollution Exposure in Lung Epithelial Cells. *Environ. Sci. Pollut. Res. Int.* **2020**, *27*, 31841–31853. [CrossRef]
10. Papaccio, F.; D′Arino, A.; Caputo, S.; Bellei, B. Focus on the Contribution of Oxidative Stress in Skin Aging. *Antioxidants* **2022**, *11*, 1121. [CrossRef]
11. Vermeij, W.P.; Alia, A.; Backendorf, C. ROS Quenching Potential of the Epidermal Cornified Cell Envelope. *J. Investig. Dermatol.* **2011**, *131*, 1435–1441. [CrossRef] [PubMed]
12. Valacchi, G.; Virgili, F.; Cervellati, C.; Pecorelli, A. OxInflammation: From Subclinical Condition to Pathological Biomarker. *Front. Physiol.* **2018**, *9*, 858. [CrossRef] [PubMed]
13. Furue, M.; Uchi, H.; Mitoma, C.; Hashimoto-Hachiya, A.; Chiba, T.; Ito, T.; Nakahara, T.; Tsuji, G. Antioxidants for Healthy Skin: The Emerging Role of Aryl Hydrocarbon Receptors and Nuclear Factor-Erythroid 2-Related Factor-2. *Nutrients* **2017**, *9*, 223. [CrossRef] [PubMed]
14. Parrado, C.; Mercado-Saenz, S.; Perez-Davo, A.; Gilaberte, Y.; Gonzalez, S.; Juarranz, A. Environmental Stressors on Skin Aging. Mechanistic Insights. *Front. Pharmacol.* **2019**, *10*, 759. [CrossRef]
15. Furue, M.; Hashimoto-Hachiya, A.; Tsuji, G. Antioxidative Phytochemicals Accelerate Epidermal Terminal Differentiation via the AHR-OVOL1 Pathway: Implications for Atopic Dermatitis. *Acta Derm. Venerol.* **2018**, *98*, 918–923. [CrossRef]
16. Galán-Ganga, M.; Del Río, R.; Jiménez-Moreno, N.; Díaz-Guerra, M.; Lastres-Becker, I. Cannabinoid CB2 Receptor Modulation by the Transcription Factor NRF2 Is Specific in Microglial Cells. *Cell Mol. Neurobiol.* **2020**, *40*, 167–177. [CrossRef]
17. Zhang, M.; Zhang, M.; Wang, L.; Yu, T.; Jiang, S.; Jiang, P.; Sun, Y.; Pi, J.; Zhao, R.; Guan, D. Activation of Cannabinoid Type 2 Receptor Protects Skeletal Muscle from Ischemia-Reperfusion Injury Partly via Nrf2 Signaling. *Life Sci.* **2019**, *230*, 55–67. [CrossRef]
18. McDonnell, C.; Leánez, S.; Pol, O. The Inhibitory Effects of Cobalt Protoporphyrin IX and Cannabinoid 2 Receptor Agonists in Type 2 Diabetic Mice. *Int. J. Mol. Sci.* **2017**, *18*, 2268. [CrossRef]

19. He, Y.; Jia, H.; Yang, Q.; Shan, W.; Chen, X.; Huang, X.; Liu, T.; Sun, R. Specific Activation of CB2R Ameliorates Psoriasis-Like Skin Lesions by Inhibiting Inflammation and Oxidative Stress. *Inflammation* **2023**, *46*, 1255–1271. [CrossRef] [PubMed]

20. Ibrahim, M.M.; Porreca, F.; Lai, J.; Albrecht, P.J.; Rice, F.L.; Khodorova, A.; Davar, G.; Makriyannis, A.; Vanderah, T.W.; Mata, H.P.; et al. CB2 Cannabinoid Receptor Activation Produces Antinociception by Stimulating Peripheral Release of Endogenous Opioids. *Proc. Natl. Acad. Sci. USA* **2005**, *102*, 3093–3098. [CrossRef] [PubMed]

21. Benedusi, M.; Kerob, D.; Guiotto, A.; Cervellati, F.; Ferrara, F.; Pambianchi, E. Topical Application of M89PF Containing Vichy Mineralising Water and Probiotic Fractions Prevents Cutaneous Damage Induced by Exposure to UV and O3. *Clin. Cosmet. Investig. Dermatol.* **2023**, *16*, 1769–1776. [CrossRef]

22. Vostálová, J.; Tinková, E.; Biedermann, D.; Kosina, P.; Ulrichová, J.; Rajnochová Svobodová, A. Skin Protective Activity of Silymarin and Its Flavonolignans. *Molecules* **2019**, *24*, 1022. [CrossRef]

23. Katiyar, S.K.; Meleth, S.; Sharma, S.D. Silymarin, a Flavonoid from Milk Thistle (*Silybum marianum* L.), Inhibits UV-Induced Oxidative Stress Through Targeting Infiltrating CD11b+ Cells in Mouse Skin. *Photochem. Photobiol.* **2008**, *84*, 266–271. [CrossRef] [PubMed]

24. Frankova, J.; Juranova, J.; Biedermann, D.; Ulrichova, J. Influence of Silymarin Components on Keratinocytes and 3D Reconstructed Epidermis. *Toxicol. In Vitro* **2021**, *74*, 105162. [CrossRef] [PubMed]

25. Surai, P.F. Silymarin as a Natural Antioxidant: An Overview of the Current Evidence and Perspectives. *Antioxidants* **2015**, *4*, 204–247. [CrossRef] [PubMed]

26. Vargas-Mendoza, N.; Morales-González, Á.; Morales-Martínez, M.; Soriano-Ursúa, M.A.; Delgado-Olivares, L.; Sandoval-Gallegos, E.M.; Madrigal-Bujaidar, E.; Álvarez-González, I.; Madrigal-Santillán, E.; Morales-Gonzalez, J.A. Flavolignans from Silymarin as Nrf2 Bioactivators and Their Therapeutic Applications. *Biomedicines* **2020**, *8*, 122. [CrossRef] [PubMed]

27. Pouwer, F.; van der Ploeg, H.M.; Adèr, H.J.; Heine, R.J.; Snoek, F.J. The 12-Item Well-Being Questionnaire. An Evaluation of Its Validity and Reliability in Dutch People with Diabetes. *Diabetes Care* **1999**, *22*, 2004–2010. [CrossRef] [PubMed]

28. Passeron, T.; Krutmann, J.; Andersen, M.L.; Katta, R.; Zouboulis, C.C. Clinical and Biological Impact of the Exposome on the Skin. *J. Eur. Acad. Dermatol. Venereol.* **2020**, *34*, 4–25. [CrossRef] [PubMed]

29. Martin, P.; Goldstein, J.D.; Mermoud, L.; Diaz-Barreiro, A.; Palmer, G. IL-1 Family Antagonists in Mouse and Human Skin Inflammation. *Front. Immunol.* **2021**, *12*, 652846. [CrossRef] [PubMed]

30. Yang, L.; Fan, X.; Cui, T.; Dang, E.; Wang, G. Nrf2 Promotes Keratinocyte Proliferation in Psoriasis through Up-Regulation of Keratin 6, Keratin 16, and Keratin 17. *J. Investig. Dermatol.* **2017**, *137*, 2168–2176. [CrossRef]

31. Houessinon, A.; François, C.; Sauzay, C.; Louandre, C.; Mongelard, G.; Godin, C.; Bodeau, S.; Takahashi, S.; Saidak, Z.; Gutierrez, L.; et al. Metallothionein-1 as a Biomarker of Altered Redox Metabolism in Hepatocellular Carcinoma Cells Exposed to Sorafenib. *Mol. Cancer* **2016**, *15*, 38. [CrossRef]

32. Chung, J.H.; Youn, S.H.; Koh, W.S.; Eun, H.C.; Cho, K.H.; Park, K.C.; Youn, J.I. Ultraviolet B Irradiation-Enhanced Interleukin (IL)-6 Production and mRNA Expression Are Mediated by IL-1 Alpha in Cultured Human Keratinocytes. *J. Investig. Dermatol.* **1996**, *106*, 715–720. [CrossRef]

33. Magcwebeba, T.; Riedel, S.; Swanevelder, S.; Bouic, P.; Swart, P.; Gelderblom, W. Interleukin-1a Induction in Human Keratinocytes (HaCaT): An In Vitro Model for Chemoprevention in Skin. *J. Ski. Cancer* **2012**, *2012*, e393681. [CrossRef]

34. Costantini, C.; Renga, G.; Oikonomou, V.; Paolicelli, G.; Borghi, M.; Pariano, M.; De Luca, A.; Puccetti, M.; Stincardini, C.; Mosci, P.; et al. The Mast Cell-Aryl Hydrocarbon Receptor Interplay at the Host-Microbe Interface. *Mediat. Inflamm.* **2018**, *2018*, 7396136. [CrossRef]

35. Sehra, S.; Serezani, A.P.M.; Ocaña, J.A.; Travers, J.B.; Kaplan, M.H. Mast Cells Regulate Epidermal Barrier Function and the Development of Allergic Skin Inflammation. *J. Investig. Dermatol.* **2016**, *136*, 1429–1437. [CrossRef]

36. Ständer, S.; Schmelz, M.; Metze, D.; Luger, T.; Rukwied, R. Distribution of Cannabinoid Receptor 1 (CB1) and 2 (CB2) on Sensory Nerve Fibers and Adnexal Structures in Human Skin. *J. Dermatol. Sci.* **2005**, *38*, 177–188. [CrossRef]

37. Casares, L.; García, V.; Garrido-Rodríguez, M.; Millán, E.; Collado, J.A.; García-Martín, A.; Peñarando, J.; Calzado, M.A.; De La Vega, L.; Muñoz, E. Cannabidiol Induces Antioxidant Pathways in Keratinocytes by Targeting BACH1. *Redox Biol.* **2020**, *28*, 101321. [CrossRef] [PubMed]

38. Jang, Y.S.; Jeong, S.; Kim, A.-r.; Mok, B.R.; Son, S.J.; Ryu, J.; Son, W.S.; Yun, S.K.; Kang, S.; Kim, H.J.; et al. Cannabidiol Mediates Epidermal Terminal Differentiation and Redox Homeostasis through Aryl Hydrocarbon Receptor (AhR)-Dependent Signaling. *J. Dermatol. Sci.* **2023**, *109*, 61–70. [CrossRef] [PubMed]

39. Baswan, S.M.; Klosner, A.E.; Glynn, K.; Rajgopal, A.; Malik, K.; Yim, S.; Stern, N. Therapeutic Potential of Cannabidiol (CBD) for Skin Health and Disorders. *Clin. Cosmet. Investig. Dermatol.* **2020**, *13*, 927–942. [CrossRef] [PubMed]

40. Marrot, L. Pollution and Sun Exposure: A Deleterious Synergy. Mechanisms and Opportunities for Skin Protection. *Curr. Med. Chem.* **2018**, *25*, 5469–5486. [CrossRef] [PubMed]

41. Li, Y.-R.; Li, G.-H.; Zhou, M.-X.; Xiang, L.; Ren, D.-M.; Lou, H.-X.; Wang, X.-N.; Shen, T. Discovery of Natural Flavonoids as Activators of Nrf2-Mediated Defense System: Structure-Activity Relationship and Inhibition of Intracellular Oxidative Insults. *Bioorganic Med. Chem.* **2018**, *26*, 5140–5150. [CrossRef]

42. Khan, H.; Tundis, R.; Ullah, H.; Aschner, M.; Belwal, T.; Mirzaei, H.; Akkol, E.K. Flavonoids Targeting NRF2 in Neurodegenerative Disorders. *Food Chem. Toxicol.* **2020**, *146*, 111817. [CrossRef]

43. Mendonca, P.; Soliman, K.F.A. Flavonoids Activation of the Transcription Factor Nrf2 as a Hypothesis Approach for the Prevention and Modulation of SARS-CoV-2 Infection Severity. *Antioxidants* **2020**, *9*, 659. [CrossRef]

44. Suraweera, T.L.; Rupasinghe, H.P.V.; Dellaire, G.; Xu, Z. Regulation of Nrf2/ARE Pathway by Dietary Flavonoids: A Friend or Foe for Cancer Management? *Antioxidants* **2020**, *9*, 973. [CrossRef] [PubMed]

45. Furue, M. Regulation of Filaggrin, Loricrin, and Involucrin by IL-4, IL-13, IL-17A, IL-22, AHR, and NRF2: Pathogenic Implications in Atopic Dermatitis. *Int. J. Mol. Sci.* **2020**, *21*, 5382. [CrossRef] [PubMed]

46. Lessard, J.C.; Piña-Paz, S.; Rotty, J.D.; Hickerson, R.P.; Kaspar, R.L.; Balmain, A.; Coulombe, P.A. Keratin 16 Regulates Innate Immunity in Response to Epidermal Barrier Breach. *Proc. Natl. Acad. Sci. USA* **2013**, *110*, 19537–19542. [CrossRef] [PubMed]

47. Edamitsu, T.; Taguchi, K.; Okuyama, R.; Yamamoto, M. AHR and NRF2 in Skin Homeostasis and Atopic Dermatitis. *Antioxidants* **2022**, *11*, 227. [CrossRef] [PubMed]

48. Wu, Q.; Ma, Y.; Liu, Y.; Wang, N.; Zhao, X.; Wen, D. CB2R Agonist JWH-133 Attenuates Chronic Inflammation by Restraining M1 Macrophage Polarization via Nrf2/HO-1 Pathway in Diet-Induced Obese Mice. *Life Sci.* **2020**, *260*, 118424. [CrossRef] [PubMed]

49. Li, L.; Liu, X.; Ge, W.; Chen, C.; Huang, Y.; Jin, Z.; Zhan, M.; Duan, X.; Liu, X.; Kong, Y.; et al. CB2R Deficiency Exacerbates Imiquimod-Induced Psoriasiform Dermatitis and Itch Through the Neuro-Immune Pathway. *Front. Pharmacol.* **2022**, *13*, 790712. [CrossRef]

50. Du, Y.; Ren, P.; Wang, Q.; Jiang, S.-K.; Zhang, M.; Li, J.-Y.; Wang, L.-L.; Guan, D.-W. Cannabinoid 2 Receptor Attenuates Inflammation during Skin Wound Healing by Inhibiting M1 Macrophages Rather than Activating M2 Macrophages. *J. Inflamm.* **2018**, *15*, 25. [CrossRef]

51. Atalay, S.; Jarocka-Karpowicz, I.; Skrzydlewska, E. Antioxidative and Anti-Inflammatory Properties of Cannabidiol. *Antioxidants* **2020**, *9*, 21. [CrossRef]

52. Jarocka-Karpowicz, I.; Biernacki, M.; Wroński, A.; Gęgotek, A.; Skrzydlewska, E. Cannabidiol Effects on Phospholipid Metabolism in Keratinocytes from Patients with Psoriasis Vulgaris. *Biomolecules* **2020**, *10*, 367. [CrossRef] [PubMed]

53. Gęgotek, A.; Atalay, S.; Domingues, P.; Skrzydlewska, E. The Differences in the Proteome Profile of Cannabidiol-Treated Skin Fibroblasts Following UVA or UVB Irradiation in 2D and 3D Cell Cultures. *Cells* **2019**, *8*, 995. [CrossRef] [PubMed]

54. Bíró, T.; Tóth, B.I.; Haskó, G.; Paus, R.; Pacher, P. The Endocannabinoid System of the Skin in Health and Disease: Novel Perspectives and Therapeutic Opportunities. *Trends Pharmacol. Sci.* **2009**, *30*, 411–420. [CrossRef] [PubMed]

55. Fink, B.; Matts, P.J.; D'Emiliano, D.; Bunse, L.; Weege, B.; Röder, S. Colour Homogeneity and Visual Perception of Age, Health and Attractiveness of Male Facial Skin. *J. Eur. Acad. Dermatol. Venereol.* **2012**, *26*, 1486–1492. [CrossRef]

56. Sun, Y.-H.P.; Zhang, X.; Lu, N.; Li, J.; Wang, Z. Your Face Looks the Same as before, Only Prettier: The Facial Skin Homogeneity Effects on Face Change Detection and Facial Attractiveness Perception. *Front. Psychol.* **2022**, *13*, 935347. [CrossRef]

57. Melas, P.A.; Scherma, M.; Fratta, W.; Cifani, C.; Fadda, P. Cannabidiol as a Potential Treatment for Anxiety and Mood Disorders: Molecular Targets and Epigenetic Insights from Preclinical Research. *Int. J. Mol. Sci.* **2021**, *22*, 1863. [CrossRef]